Mon. Not. R. Astron. Soc. **325,** 715–725 (2001)

Low-frequency waves in asymmetric magnetized relativistic pair plasma

M. Gedalin,[1★] E. Gruman[1] and D. B. Melrose[2]

[1]*Ben-Gurion University, Beer-Sheva 84105, Israel*

[2]*Research Centre for Theoretical Astrophysics, School of Physics, University of Sydney, NSW 2006, Australia*

Accepted 2001 March 5. Received 2001 February 15; in original form 2000 December 4

ABSTRACT

The properties of waves in a pulsar magnetosphere are considered in the most general case of a non-neutral, current-carrying pair plasma with arbitrary distribution functions for electrons and positrons. General dispersion relations are derived for a strong but finite magnetic field, including gyrotropic terms caused by the deviations from quasi-neutrality and the relative streaming of electrons and positrons. It is shown how the ellipticity of the wave polarization depends on the plasma parameters and angle of propagation. Two examples of plasma distributions are analysed numerically: a waterbag distribution and a piecewise distribution that models the numerical result for pair cascades. A possible application to the interpretation of the observed circular polarization of some pulsars is discussed.

Key words: magnetic fields – plasmas – waves – pulsars: general.

1 INTRODUCTION

The pulsed non-thermal radio emission of pulsars is believed to be generated in the relativistic pair plasma, filling the polar cap regions of the pulsar magnetosphere (e.g. Manchester & Taylor 1977). This plasma is produced via electromagnetic cascade (Arons 1983 and references therein) in a superstrong magnetic field. In most models (Melrose 1993) the density of the pair plasma N_p exceeds, by several orders of magnitude, the Goldreich–Julian density $N_{GJ} = \boldsymbol{B}\cdot\boldsymbol{\Omega}/2\pi ec$ (where $\boldsymbol{B}$ is the magnetic field and $\boldsymbol{\Omega}$ is the angular velocity of the pulsar), although the multiplicity factor $M = N_p/N_{GJ} \gg 1$ is poorly known (Shibata, Miyazaki & Takahara 1998). The primary plasma (which is the source of the denser secondary plasma) is of density $\sim N_{GJ}$ and flows along the field lines with the Lorentz-factor $\gamma_{pr} \sim 10^7$. The parameters for the secondary plasma are poorly constrained. An estimate considered plausible is a flow Lorentz-factor $\gamma_p \sim \gamma_{pr}/M$ (Arons 1983; Melrose 1993; Shibata et al. 1998) with a spread $\langle\gamma\rangle \sim \gamma_p$ in the rest frame of the plasma.

The necessity to screen out the corotational electric field (Manchester & Taylor 1977) requires that the pair plasma have a non-zero charge density $N_+ - N_- = N_{GJ}$. The primary beam (Ruderman & Sutherland 1975) carries a current, and current conservation requires that this current be carried outwards through the secondary plasma (Lyutikov 1998). On the other hand, the condition $N_+ - N_- = N_{GJ}$ also requires a backward-flowing current (Lyubarskii 1992).

The properties of the waves in pair plasma in the emission region and above it along the path of the ray are thought to play a significant role in influencing some features of the observed radio emission (e.g. Melrose 1995 and references therein). In particular, the pair plasma is thought to produce the outgoing radio waves (in the10^8–10^{10} Hz frequency range) through some form of plasma instability. Cyclotron (Lominadze, Machabeli & Usov 1983), curvature (e.g., Lyutikov 1999 and references therein) and beam (Lominadze, Mikhailovskii & Sagdeev 1979; Usov 1987; Lyubarskii 1992) instabilities have been proposed. The particle energy is then either transformed directly into radio waves which are capable of escaping from the pulsar magnetosphere, or into waves that cannot themselves escape but which produce the escaping radio waves through some additional, probably non-linear mechanism (Melrose 1993, 1995). In any case the features of the waves in the pair plasma are of crucial importance for understanding the radio emission mechanism.

Waves in a pair plasma with identical distributions of electrons and positrons have been studied extensively (Lominadze et al. 1979; Gedalin & Machabeli 1982; Volokitin, Krasnoselskikh & Machabeli 1985; Arons & Barnard 1986; Lyubarskii 1995; Gedali, Melrose & Gruman 1998; Melrose et al. 1999; Han, Manchester & Qiao 2000) in the cold as well as in the hot regimes. For identical distributions of electrons and positrons the wave polarization is strictly linear. When the distributions are not identical the wave modes have a non-zero circular component that is of interest for the interpretation of the observed polarization. The radio emission is well known to be typically highly, linearly polarized, and it is now well established that many pulsars also have a substantial circular polarization (Han et al. 1998; Manchester, Han & Qiao 1998; von Hoensbroech, Kijak & Krawczyk 1998; von Hoensbroech & Lesch 1999; Han et al. 2000). Various suggestions for the cause of circular polarization have been proposed. Specific suggestions use wave mode coupling caused by rotation (Radhakrishnan & Rankin 1990; Lyubarskii & Petrova 1999), refer to specific characteristics

★E-mail: gedalin@bgumail.bgu.ac.il

© 2001 RAS

of the emission mechanism (Gil & Snakowski 1990a,b; Radhakrishnan & Rankin 1990; Gangadhara 1997; Lyutikov, Machabeli & Blandford 1999), consider propagation effects (Petrova & Lyubarskii 2000), or invoke non-linear interactions (Lyutikov 1999). Cheng & Ruderman (1977) and later Arons & Barnard (1986) suggested that the polarization may be associated with the properties of the natural wave modes in the plasma. The ellipticity of the waves in a pair plasma is non-zero if the plasma is non-neutral or if it carries a current along the magnetic field. Wave properties in a current-carrying, relativistic pair plasma have been considered by Lyutikov (1998) for the special case where the plasma is neutral in its rest frame with a relativistic thermal (Jüttner) distribution.

In the present paper, we study the effects of non-zero charge and current densities on the wave properties in a strongly magnetized, highly relativistic pair plasma with arbitrary distribution functions for electrons and positrons. We do not assume that the charge density vanishes in either the pulsar frame or in the plasma rest frame. (Zero charge density and non-zero current density in one frame imply non-zero charge and current densities in the other frame.) We show that these conditions imply that waves with phase speed close to the speed of light can be substantially elliptically polarized. We study the dependence of the elliptical polarization on the plasma parameters. We illustrate the analysis with two numerical examples of different distributions. One is a waterbag distribution: it has been shown (Gedalin et al. 1998; Melrose et al. 1999) that this provides a semi-quantitative correct description of the wave features apart from their damping rates. The other distribution that we choose is a piecewise continuous model for the distributions found in pair cascade calculations (Daugherty & Harding 1982).

In Section 2 we describe the plasma conditions from the point of view of the pulsar and plasma rest frames. The general dielectric tensor and dispersion relation are given in Section 3. The wave features in the infinite magnetic field limit are summarized in Section 4. The generalization to a finite magnetic field, including wave polarization, is considered in Section 5. The dielectric tensor is evaluated for the waterbag distribution in Section 6. In Section 7 we present results for the distribution that simulates the results of pair cascade calculations (Daugherty & Harding 1982). We discuss the results in Section 9.

2 PULSAR CONDITIONS

The plasma which fills the pulsar magnetosphere is produced in a electromagnetic cascade, beginning most probably with acceleration of (primary) charge particles along the magnetic field lines in the polar gap up to very high energies of $\gamma_{\rm pr} \sim 10^7$. While moving along the curved magnetic field lines the primary particles emit high-energy curvature photons that, in turn, produce electron–positron plasma pairs. Alternatively, the high-energy photons may be produced by Compton scattering of thermal photons from the polar cap surface (Zhang & Harding 2000). This copious pair production develops in an explosive way, and a relativistic dense plasma is produced in a narrow layer known as the pair production front (Arons 1983), behind which a dense secondary plasma is formed. It had been thought that this dense secondary plasma would screen out the parallel electric field, but serious doubts have been raised as to whether this is possible (Shibata et al. 1998).

The secondary plasma parameters depend on the details of the polar cap structure, in particular, on the electric field, the height of the acceleration region and the geometry of the magnetic field [which affects both the generation of the curvature photons and also the details of the secondary pair production (Arons 1983)]. The density of primary particles just below the pair production front is assumed to be $N_{\rm pr} \sim N_{\rm GJ}$. The secondary plasma density is written as $N_{\rm p} \sim MN_{\rm GJ}$, where the multiplicity factor $M \sim 10^2$–10^5 is poorly determined (Lyutikov 1998; Shibata et al. 1998). For the sake of discussion we assume $\gamma_{\rm p} \sim \gamma_{\rm pr}/M$ for the Lorentz-factor of the secondary plasma *bulk flow* in the pulsar frame.

In what follows we use the following notation: all variables measured in the pulsar frame are primed, and non-primed variables refer to the *plasma* rest frame (not necessarily the zero-bulk flow frame) moving with the Lorentz-factor $\gamma_{\rm p}$. We use the spatial component of the 4-velocity $\boldsymbol{u} = \gamma\boldsymbol{v}/c$ (the definition is valid in both frames), so that, for motion strictly along the magnetic field lines, the transformation rules are

$$u' = \gamma_{\rm p} u + u_{\rm p}\gamma, \qquad \gamma' = \gamma_{\rm p}\gamma + u_{\rm p} u, \tag{1}$$

$$u = \gamma_{\rm p} u' - u_{\rm p}\gamma', \qquad \gamma = \gamma_{\rm p}\gamma' - u_{\rm p} u', \tag{2}$$

where $\gamma = \sqrt{1+u^2}$ (for the primed and p-subscripted variables, respectively). The invariance of the distribution function implies $f'(u') = f(u)$.

The production mechanism for the secondary pair plasma implies a distribution function in the pulsar frame that is limited by some $u'_{\rm min} \gtrsim 1$ from below and by some $u'_{\rm max}$ from above. The 4-speed $u'_{\rm max}$ is thought to be greater than the average $\langle u' \rangle$ by about an order of magnitude, where it is assumed that the distribution decreases rapidly with energy and that $u_{\rm p}$ is high. The corresponding limits in the plasma frame i.e. $u_{\rm min}$ and $u_{\rm max}$ depend on $\gamma_{\rm p}$, namely, $u_{\rm max}$ increases with increasing Lorentz-factor of the flow. This is illustrated by Fig. 1 where the distribution function $f(u) = {\rm const}\,\gamma^{-3/2}$, $|u| < u_{\rm max}$ is transformed from the plasma rest frame into the pulsar frame. For $u_{\rm max} = -u_{\rm min} = 1$ and $u_{\rm p} = 20$ the distribution in the pulsar frame is limited by $u'_{\rm min} \approx 8$ and $u'_{\rm max} \approx 48$. For $u_{\rm max} = -u_{\rm min} = 1$ and $u_{\rm p} = 2000$ the limits are $u'_{\rm min} \approx 800$ and $u'_{\rm max} \approx 4800$, while choosing $u_{\rm max} = -u_{\rm min} = 10$ with the same $u_{\rm p} = 2000$ one gets $u'_{\rm min} \approx 100$ and $u'_{\rm max} \approx 40\,000$. For large multiplicities of $M \sim 10^4$–10^5, one has $u_{\rm p} \sim 10^2$ so that in the plasma frame $u_{\rm max} \sim 1$–10.

For a pulsar with a period of $P = 0.2$ s and magnetic field on the pole $B = 10^{12}$ G (Lyutikov 1998), the Goldreich–Julian density at the pulsar surface in the polar region is $N_{\rm GJ} \approx 3.5 \times 10^{11}\,{\rm cm}^{-3}$. If the multiplicity $M \sim 10^5$ (the densest case considered), the plasma density in the pulsar frame is $N' = MN_{\rm GJ} = 3.5 \times 10^{16}\,{\rm cm}^{-3}$. For $\gamma_{\rm p} \sim 10^7 M^{-1} \sim 10^2$ the plasma density in the plasma rest frame is $N \approx N'/\gamma_{\rm p} \approx 3.5 \times 10^{14}\,{\rm cm}^{-3}$, which gives the plasma rest frame frequency of about $\omega_{\rm p} = \sqrt{4\pi N e^2/m} \approx \times 10^{12}\,{\rm s}^{-1}$. Thus, the ratio (see below) $(\omega_{\rm p}/\Omega)^2 \approx 10^{-14}(R/R_{\rm P})^3$ (plasma rest frame), where $\Omega = eB/mc$ is the gyrofrequency, R is the radius, and $R_{\rm P}$ is the pulsar radius. For the light cylinder, $R = R_{\rm L} = cP/2\pi \approx 10^3 R_{\rm P}$, the ratio $(\omega_{\rm p}/\Omega)^2 \sim 10^{-5}$. For lower multiplicities, the plasma density in the plasma frame given by $N \propto M/\gamma_{\rm p} \propto M^2$ may be lower by 2–5 orders of magnitude.

The deviations from quasi-neutrality in the pulsar frame imply $\rho'/N'e \sim 1/M$ (Manchester & Taylor 1977). The current density is also determined by the same parameter $j'/N'ec \sim 1/M$ (Lyubarskii 1992; Lyutikov 1998). The charge density and current density in the plasma rest frame may be obtained from the following transformation rules:

$$\rho' = \gamma_{\rm p}\rho + u_{\rm p} j/c, \qquad j'/c = \gamma_{\rm p} j/c + u_{\rm p}\rho, \tag{3}$$

$$\rho = \gamma_{\rm p}\rho' - u_{\rm p} j'/c, \qquad j/c = \gamma_{\rm p} j'/c - u_{\rm p}\rho', \tag{4}$$

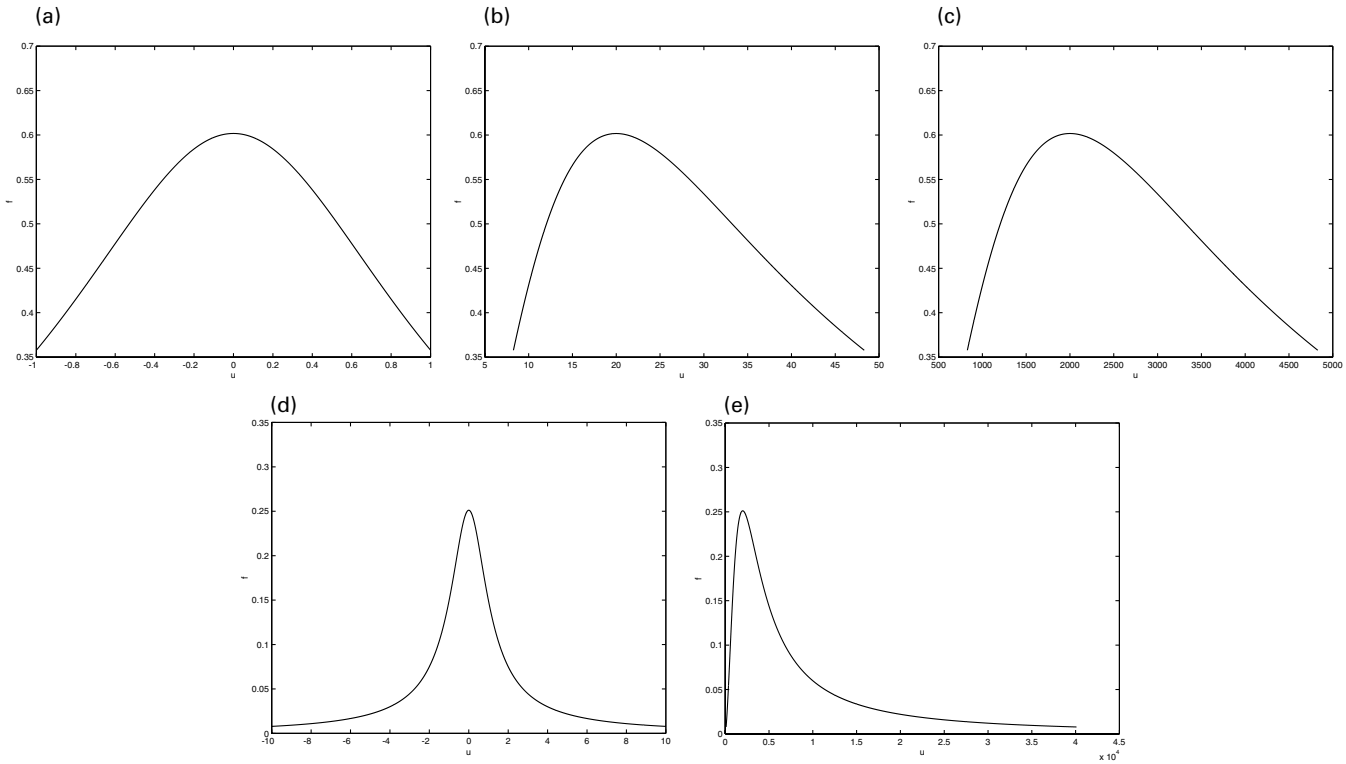

Figure 1. Transformation of the distribution of $f(u) \propto \gamma^{-3/2}$ from the plasma [(a) and (c)] to the pulsar [(b), (c), and (e)] rest frame. The parameters are chosen as follows; for (a) and (b) $u_{\max} = -u_{\min} = 1$, $u_{\rm p} = 20$; for (c) $u_{\max} = -u_{\min} = 1$, $u_{\rm p} = 2000$; for (d) and (e) $u_{\max} = -u_{\min} = 10$, $u_{\rm p} = 2000$.

and depend strongly on the details of the density and current distribution. For example, if $j'/c = \rho' v_{\rm p}/c = \rho' u_{\rm p}/\gamma_{\rm p}$ (all the current is due to the convection of the two plasma species with different densities), then in the plasma frame $\rho = \rho'/\gamma_{\rm p}$, and $j = 0$. More generally, for $j'/\rho' v_{\rm p} = \alpha$, one has

$$\rho = [\gamma_{\rm p}(1-\alpha) + \alpha/\gamma_{\rm p}]\rho', \tag{5}$$

$$j/c = (\alpha - 1)u_{\rm p}\rho'. \tag{6}$$

The assumption of Lyutikov (1998) that $\rho = 0$ corresponds to $j'/c = \gamma_{\rm p}\rho'/u_{\rm p}$ or $\alpha = c^2/v_{\rm p}^2$ also means that the current in the plasma frame $j = j'/\gamma_{\rm p}$ is weak. It is not clear as to what might ensure the fine tuning $j'/c = \gamma_{\rm p}\rho'/u_{\rm p}$ throughout the pulsar magnetosphere. In general, if α is not close to unity, the ratio of the density to the current in the plasma frame given by $\rho/Ne \sim j/Nec \sim \gamma_{\rm p}^2/M$ and can well be large.

3 DISPERSION RELATION AND WAVE PROPERTIES

The dispersion relation is obtained from the matrix equation

$$\begin{pmatrix} n_\parallel^2 - \epsilon_{xx} & -\epsilon_{xy} & -n_\parallel n_\perp - \epsilon_{xz} \\ -\epsilon_{yx} & n^2 - \epsilon_{yy} & -\epsilon_{yz} \\ -n_\parallel n_\perp - \epsilon_{zx} & -\epsilon_{zy} & n_\perp^2 - \epsilon_{zz} \end{pmatrix} \begin{pmatrix} E_x \\ E_y \\ E_z \end{pmatrix} = 0, \tag{7}$$

where $n = kc/\omega$ is the refraction index, $n_\parallel = n\cos\theta$, $n_\perp = n\sin\theta$, and θ is the angle between $\boldsymbol{k}$ and $\boldsymbol{B}_0$, here $\boldsymbol{B}_0 = (0, 0, \boldsymbol{B}_0)$ and $\boldsymbol{k} = (\boldsymbol{k}_\perp, 0, \boldsymbol{k}_\parallel)$ are the external magnetic field and wave vector, respectively. The dielectric tensor $\boldsymbol{\epsilon_{ij}}$ is determined by the plasma distribution function. The methods to calculate the dielectric tensor are well-known and can be found elsewhere (e.g. Gedalin et al. 1998). For our present purpose we use the expressions derived by Gedalin et al. (1998) for the case of a one-dimensional distribution function $f = f(u_z)\delta(u_\perp)/u_\perp$ [cf. also Lyutikov (1998), Melrose et al. (1999)]:

$$\epsilon_{xx} = \epsilon_{yy} \equiv \epsilon_\perp = 1 + \sum_s \frac{\omega_{\rm ps}^2}{\Omega_s^2}\left(\langle\gamma\rangle_s - 2n_\parallel\langle u_z\rangle_s + n_\parallel^2\langle u_z^2\gamma^{-1}\rangle_s\right), \tag{8}$$

$$\epsilon_{zz} \equiv \epsilon_\parallel = 1 - \sum_s \frac{\omega_{\rm ps}^2}{\omega^2} W_s(n_\parallel) + \sum_s \frac{\omega_{\rm ps}^2 n_\perp^2}{\Omega_s^2}\langle u_z^2\gamma^{-1}\rangle_s, \tag{9}$$

$$\epsilon_{xy} = -\epsilon_{yx} = -{\rm i}\sum_s \frac{\omega_{\rm ps}^2}{\omega\Omega_s}\left(1 - n_\parallel\langle u_z\gamma^{-1}\rangle_s\right), \tag{10}$$

$$\epsilon_{yz} = -\epsilon_{zy} = -{\rm i}\sum_s \frac{\omega_{\rm ps}^2 n_\perp}{\omega\Omega_s}\langle u_z\gamma^{-1}\rangle, \tag{11}$$

$$\epsilon_{xz} = \epsilon_{zx} \equiv Q = \sum_s \frac{\omega_{\rm ps}^2 n_\perp}{\Omega_s^2}\left(\langle u_z\rangle_s - n_\parallel\langle u_z^2\gamma^{-1}\rangle_s\right). \tag{12}$$

[The corresponding expressions of Gedalin et al. (1998) lost γ^{-1} in ϵ_{yz}.] Here $u_z = v_z/\gamma c$, $\gamma = \sqrt{1 + u_z^2}$, and averaging is defined as follows:

$$\langle\ldots\rangle = \int(\ldots)f_0(u_z)\,{\rm d}u_z, \tag{13}$$

where $f_0(u_z)$ is the equilibrium (unperturbed) distribution. The subscript s denotes summation over the plasma species (electrons and positrons). Other parameters are defined as usual: the gyrofrequency $\Omega_s = q_s B_0/m_s c$, and the plasma frequency

$\omega_{ps}^2 = 4\pi N_s q_s^2/m_s$. Equations (8)–(12) take into account both a non-zero charge density and a non-zero current density. The function W_s is defined by the integral

$$W_s(n_\parallel) = -\frac{1}{n_\parallel}\int \frac{1}{1 - n_\parallel v_z + \mathrm{i}\tau}\frac{\mathrm{d}f_{0s}}{\mathrm{d}u_z}\mathrm{d}u_z, \tag{14}$$

with $\tau \to 0$.

The off-diagonal terms vanish identically when the distribution functions of the electrons and positrons are the same, $f_+ = f_-$. We introduce the following notation:

$$N_+ = N_0(1+\eta), \qquad N_- = N_0(1-\eta), \tag{15}$$

$$m_1 = \sum_s (1+s\eta)\langle\gamma\rangle_s, \tag{16}$$

$$m_2 = \sum_s (1+s\eta)\langle u_z\rangle_s, \tag{17}$$

$$m_3 = \sum_s (1+s\eta)\langle u_z^2\gamma^{-1}\rangle, \tag{18}$$

$$W = \sum_s (1+s\eta)W_s, \tag{19}$$

$$\delta_1 = \sum_s (1+s\eta) = 2\eta, \tag{20}$$

$$\delta_2 = \sum_s s(1+s\eta)\langle u_z\gamma^{-2}\rangle, \tag{21}$$

where $s = \pm 1$. Then the dielectric tensor takes the following form:

$$\epsilon_\perp = 1 + \Delta m_1 - 2\Delta m_2 n\cos\theta + \Delta m_3 n^2\cos^2\theta, \tag{22}$$

$$\epsilon_\parallel = 1 + \Delta m_3 n^2\sin^2\theta - Z^{-2}W, \tag{23}$$

$$\epsilon_{xy} = \mathrm{i}\sqrt{\Delta}(\delta_2 n\cos\theta - \delta_1)Z^{-1}, \tag{24}$$

$$\epsilon_{xz} = \Delta m_2 n\sin\theta - \Delta m_3 n^2\sin\theta\cos\theta, \tag{25}$$

$$\epsilon_{yz} = -\mathrm{i}\sqrt{\Delta}\delta_2 n\sin\theta Z^{-1}, \tag{26}$$

where $\Delta = \omega_p^2/\Omega^2$, $\omega_p^2 = 4\pi N_0 e^2/m$, $Z = \omega/\omega_p$, $\delta_1 = \rho/N_0 e$ and $\delta_2 = j/N_0 ec$. These equations are equally valid in both the pulsar and plasma frames, provided the corresponding distribution functions are used for average calculations. In the *zero-bulk mass-flow* frame one has $m_2 = 0$. However, it is not always convenient to work in this frame, so for the time being we leave $m_2 \neq 0$, in general.

4 INFINITE MAGNETIC FIELD LIMIT

We start our analysis of the wave features with the infinite magnetic field limit where $\Delta = 0$. There are two branches (e.g. Gedalin et al. 1998): the electromagnetic t branch with the dispersion relation $n^2 = 1$, and the mixed LA (Langmuir–Alfvén) branch with the dispersion relation

$$\frac{\omega^2}{\omega_p^2} = \frac{(n_\parallel^2 - 1)W}{n^2 - 1}.$$

One has $W(n_\parallel) > 0$ for $n_\parallel < 1$, so there is only one wave in this range, namely the superluminal L mode with $n^2 < 1$. We are particularly interested in the oblique wave with $|n^2 - 1| \ll 1$. If $n_\parallel \ll 1$ one has $W = \langle\gamma^{-3}\rangle \equiv 1/\gamma^*$. We can use this expression for W in the whole range of $n_\parallel < 1$, bearing in mind the (relatively weak) dependence of γ^* on $n_\parallel$. For the L mode one has $\omega^2 = \omega_p^2/\gamma^*$ at $n = 0$, and $n^2 = 1 - \omega_p^2\sin^2\theta/\omega^2\gamma^*$ in the high-frequency limit, except when $\theta \approx 0$.

If the distributions are compact, that is, if there exists u_m such that $F = 0$ for $|u_z| > u_m$, then the A-wave is undamped in the range $1 < n_\parallel^2 < 1/v_m^2$, where $v_m^2 = u_m^2/(1+u_m^2)$. We do not further analyse the infinite magnetic field here and refer the reader to earlier studies (Lominadze et al. 1979; Gedalin & Machabeli 1982; Volokitin et al. 1985; Arons & Barnard 1986; Lyubarskii 1995; Gedalin et al. 1998; Melrose et al. 1999; Petrova & Lyubarskii 2000). Here we only mention that all modes are linearly polarized (either $E_y \neq 0$ for the t-branch, of $E_x \neq 0$ and $E_z \neq 0$ for the LA branch) in the infinite magnetic field limit.

5 FINITE MAGNETIC FIELD

If the magnetic field is not infinite, the complete dispersion equation does not split into two separate equations, and all three components of the electric field are, in general, present in the wave. The dispersion relation may be written in the form

$$A_2 Z^4 + A_1 Z^2 + A_0 = 0, \tag{28}$$

where

$$A_2 = d_{22}(d_{11}d_{33} - d_{13}^2), \tag{29}$$

$$A_1 = d_{11}d_{22}W - d_{11}d_{23}^2 - d_{33}d_{12}^2 + 2d_{12}d_{23}d_{13}, \tag{30}$$

$$A_0 = -Wd_{12}^2, \tag{31}$$

$$d_{11} = n^2\cos^2\theta(1 - \Delta m_3) + 2n\cos\theta\Delta m_2 - (1 + \Delta m_1), \tag{32}$$

$$d_{22} = n^2(1 - \Delta m_3\cos^2\theta) + 2n\cos\theta\Delta m_2 - (1 + \Delta m_1), \tag{33}$$

$$d_{13} = -n^2\sin\theta\cos\theta(1 - \Delta m_3) - n\sin\theta\Delta m_2, \tag{34}$$

$$d_{12} = \sqrt{\Delta}(n\cos\theta\delta_2 - \delta_1), \tag{35}$$

$$d_{23} = \sqrt{\Delta}n\sin\theta\delta_2, \tag{36}$$

and

$$d_{33} = n^2\sin^2\theta(1 - \Delta m_3) - 1. \tag{37}$$

The polarization ratios are given by

$$r_x \equiv \frac{E_x}{|\boldsymbol{E}|} = (d_{12}d_{23} - Z^2 d_{22}d_{13})/D, \tag{38}$$

$$r_y \equiv \frac{\mathrm{i}E_y}{|\boldsymbol{E}|} = Z(d_{11}d_{23} - d_{12}d_{13})/D, \tag{39}$$

$$r_z \equiv \frac{E_z}{|\boldsymbol{E}|} = (Z^2 d_{11}d_{22} - d_{12}^2)/D \tag{40}$$

where

$$D = [(d_{12}d_{23} - Z^2 d_{22}d_{13})^2 + Z^2(d_{11}d_{23} - d_{12}d_{13})^2 + (Z^2 d_{11}d_{22} - d_{12}^2)^2]^{1/2}. \tag{41}$$

Non-zero r_y implies non-zero elliptical polarization. For an almost electromagnetic (transverse) wave, $r_y \approx \sqrt{2} \approx 0.7$ would mean nearly circular polarization. As $d_{11}d_{23} - d_{12}d_{13} \propto \sqrt{\Delta}\delta \ll 1$, the only way to have substantial elliptical polarization is to require $d_{22} \approx 0$, that is, $|n^2 - 1| \ll 1$, which, in turn, is possible only for $Z \gg 1$.

Let us consider the dispersion relation given by equation (28) in the pulsar frame in greater detail. We are interested in the waves which do not damp on the Cerenkov resonance. In the case of an exponentially decreasing distribution, such as a relativistic thermal (Jüttner) distribution, it is sufficient to require that $n_\parallel\langle v_z\rangle < 1$

(Lyutikov 1998) to satisfy the weak cyclotron damping condition. However, for the power law spectrum (Daugherty & Harding 1982) or flat distribution (Arons & Barnard 1986) one has to require that either $n_\parallel v_{\max} < 1$ or $n_\parallel v_{\min} > 1$ (Gedalin et al. 1998). The low-frequency long-wavelength limit (far below the cyclotron resonance) condition is stricter: $\gamma|1 - n\cos\theta v| \ll \Omega/\omega$. If the polarization forms at $R \sim 10^3 R_{\rm P}$ (Cheng & Ruderman 1977) then $\Omega \sim 10^{10}$–$10^{11}\,{\rm s}^{-1}$, while the observed radio frequencies are in the range of 10^9–$10^{11}\,{\rm s}^{-1}$, so that $\omega/\Omega \lesssim 1$. Together with the previous condition, this gives either $-1/\gamma_{\max} \ll n_\parallel - 1 \lesssim 1/2\gamma_{\max}^2$ or $1/2\gamma_{\min}^2 \lesssim n_\parallel - 1 \ll 1/2\gamma_{\max}$. For $\gamma_{\min} = \gamma_1 \approx 10$ and $\gamma_{\max} = \gamma_4 \approx 10^3$ the second condition cannot be satisfied. We therefore restrict ourselves with the range $-1/\gamma_{\max} \lesssim n_\parallel - 1 \lesssim 1/2\gamma_{\max}^2$.

From the previous analysis it is clear that we are interested in the range of $\theta \ll 1$ and $n \approx 1$. Let us define $n_\parallel = 1 + \chi$, where $|\chi| \ll 1$. Expanding and retaining the leading terms in small parameters χ, θ, and Δ, one finds $d_{11} = 2(\chi - \chi_1)$, $d_{22} = -d_{11}d_{33} + d_{13}^2 = \chi - \chi_2$, where $\chi_1 = \Delta(m_1 + m_3 - 2m_2)/2$, $\chi_2 = \chi_1 - \theta^2/2$. Let us first consider the case of the symmetric plasma given by $d_{12} = 0$, $d_{23} = 0$. Then the dispersion relation given by equation (28) splits into two separate dispersion relations:

$$\chi = \chi_2, \tag{42}$$

$$Z^2 = \frac{W(\chi - \chi_1)}{\chi - \chi_2}. \tag{43}$$

The second dispersion relation describes the L mode (asymptotically approaching $\chi = \chi_2$) and the A mode, whose frequency is limited from above (cf. Gedalin et al. 1998) in view of the requirement $\chi \lesssim 1/2\gamma_{\max}^2$. The A mode is not of any interest to us and is not mentioned further.

For the L mode in the high-frequency range one has from equation (43)

$$\chi = \chi_2 - \frac{W\theta^2}{Z^2}. \tag{44}$$

As $W \lesssim \langle\gamma\rangle$, the difference between $n_\parallel$ for t (see equation 42) and L modes is small at high frequencies and small angles.

Let us now analyse the complete dispersion relation given by equation (28). To leading order in small quantities it can be written as

$$4Z^2\,(Z^2 - W)(\chi - \chi_2)^2 + 2\theta^2 W(\chi - \chi_2) - (Z^2 - W)\Delta(\delta_2 - \delta_1)^2 = 0. \tag{45}$$

The solutions are

$$\chi - \chi_2 = \frac{-\theta^2 W Z^2 \pm \sqrt{\theta^4 W^2 Z^4 + 4(Z^2 - W)Z^2\Delta(\delta_2 - \delta_1)^2}}{4Z^2(Z^2 - W)}. \tag{46}$$

The refraction index is obtained as $n = n_\parallel/\cos\theta = 1 + \chi + \theta^2/2$ in the same approximation. Equation (46) can be used in equations (38) and (39) to obtain

$$\left|\frac{E_y}{E_x}\right| = \frac{2Z^2|\chi - \chi_2|}{\sqrt{\Delta}Z|\delta_2 - \delta_1|}. \tag{47}$$

Equations (46) and (47) provide the general solution for the wave properties, albeit in implicit form as a result of W being a function of $n_\parallel$. Unfortunately, there is no universal approximation for W in the range $-1/2\gamma_{\max} < \chi < 1/2\gamma_{\max}^2$, so these relations are of limited use. On the other hand, equation (28) together can be considered as a parametric representation of $\omega/\omega_{\rm p} = Z(n)$ and $kc/\omega_{\rm p} = nZ(n)$. Then equations (38)–(40) give the polarization features in the parametric form. In the next two sections we illustrate the use of this parametric representation with two different distributions considered in the plasma (waterbag distribution; Arons & Barnard 1986) and (pulsar power-law distribution; Daugherty & Harding 1982) rest frames. Equation (28) is solved with respect to Z, and W is calculated analytically (for the waterbag distribution) or determined numerically (for the power-law distribution).

6 EXAMPLE 1: WATERBAG DISTRIBUTION IN THE PLASMA FRAME

In this section we consider the waterbag distribution in the plasma frame. Such a distribution was first proposed as an approximation by Arons & Barnard (1986) and roughly corresponds to their described pair distribution transformed into the plasma frame. To take into account the non-zero charge and current densities, we consider the waterbag distributions for electrons and positrons that are shifted one relative to one another as

$$f_+ = \frac{1 + \eta}{u_1 + u_2}\Theta(u_2 - u_z)\Theta(u_1 + u_z), \tag{48}$$

$$f_- = \frac{1 - \eta}{u_1 + u_2}\Theta(u_2 + u_z)\Theta(u_1 - u_z). \tag{49}$$

These shifted waterbag distributions allow an exact calculation of the dispersion relation in the form of algebraic equations, which greatly simplifies the analysis. We expect that the analysis will describe properly the features of the modes in the asymmetric relativistic pair plasma. Gedalin et al. (1998) have shown that more realistic distribution functions add dissipation to the waves with the phase velocities $\omega/k_\parallel < u_-$, prohibiting propagation of waves with very low phase velocities (too large $n > n_m$, where n_m is determined by the distribution function, $n_m = 1/v_m$ for the compact distribution). At the same time in the high-phase velocity range, with $n < n_m$, the wave features do not depend significantly on the exact form of the distribution, and usage of the waterbag distribution is justified and instructive.

With these waterbag distributions one finds:

$$m_1 = \{u_1\gamma_1 + u_2\gamma_2 + \ln[(\gamma_1 + u_1)(\gamma_2 + u_2)]\}(u_1 + u_2)^{-1}, \tag{50}$$

$$m_2 = \eta(u_2 - u_1), \tag{51}$$

$$m_3 = \left[\frac{u_1\gamma_1 + u_2\gamma_2}{2} - \frac{1}{2}\ln\left(\frac{\gamma_1 + u_1}{\gamma_2 - u_2}\right)\right](u_1 + u_2)^{-1}, \tag{52}$$

$$\delta_1 = 2\eta, \tag{53}$$

$$\delta_2 = 2(\gamma_2 - \gamma_1)/(u_1 + u_2), \tag{54}$$

$$W = \frac{2}{u_1 + u_2}\left(\frac{v_1}{1 - n^2\cos^2\theta v_1^2} + \frac{v_2}{1 - n^2\cos^2\theta v_2^2}\right) + \frac{\eta n\cos\theta(v_2^2 - v_1^2)}{(u_1 + u_2)(1 - n^2\cos^2\theta v_1^2)(1 - n^2\cos^2\theta v_2^2)}. \tag{55}$$

Equations (53)–(55) are used below for the graphical presentation of the polarization. Being particularly interested in circular (elliptical) polarization, we use the ratio $r_y = {\rm i}E_y/\sqrt{E_x^2 + E_y^2 + E_z^2}$ as the signature of ellipticity (E_x and E_z are in phase and are chosen to be real, so that ${\rm i}E_y$ is also real).

Fig. 2 shows the ellipticity as a function of frequency for several different angles of propagation i.e. for $\theta = 1°$, $2°$, and $5°$. Only one

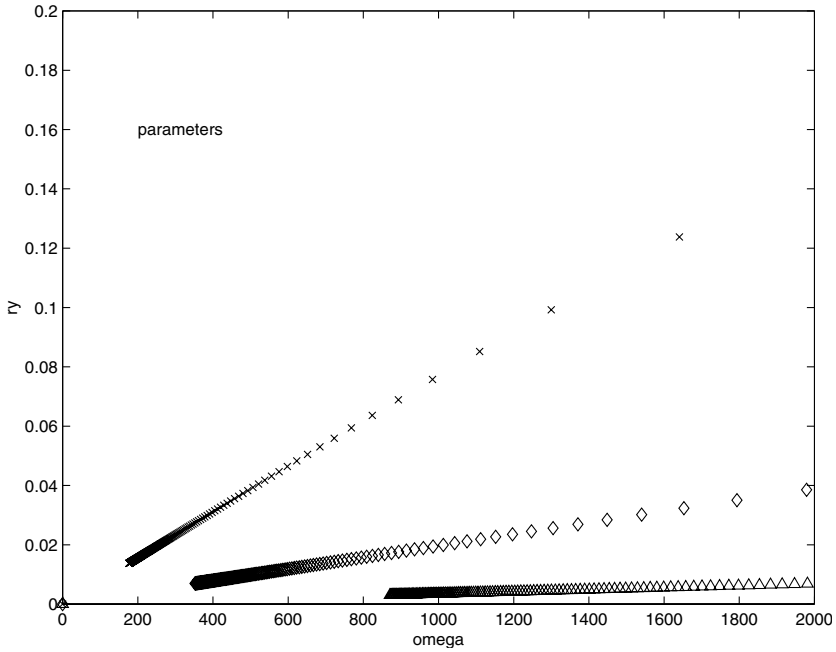

Figure 2. Ellipticity for $\Delta = 10^{-8}$, $u_0 = 2$, $\bar{u} = 0.01$, $\eta = 0.005$, and different propagation angles $\theta = 1°$ (crosses), 2° (diamonds), and 5° (triangles), as a function of frequency.

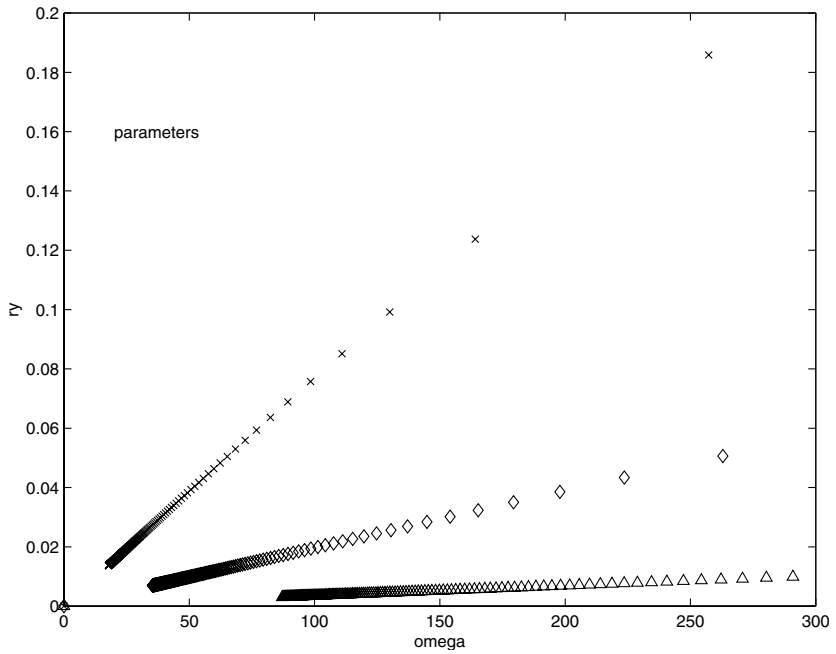

Figure 3. Ellipticity for $\Delta = 10^{-6}$, $u_0 = 2$, $\bar{u} = 0.01$, $\eta = 0.005$, and different propagation angles $\theta = 1°$ (crosses), 2° (diamonds), and 5° (triangles), as a function of frequency.

mode is shown for clarity. The plasma parameters chosen are: $\Delta = 10^{-8}$, $u_0 = 2$, $\bar{u} = 0.01$, $\eta = 0.005$, which corresponds to $\delta_1 = 0.01$ and $\delta_2 = 0.009$. The ellipticity r_y rapidly decreases to nearly zero as the propagation angle increases. At small angles the ellipticity is still not negligible, despite the very small parameter Δ. The ellipticity increases with increasing frequency. It should be noted that only the range $\omega/\omega_p \ll \sqrt{1/\Delta}$ is of physical significance because of the initial assumption that $|\omega - k_z v_z| \ll \Omega\langle\gamma\rangle$. That means that only the range $\omega/\omega_p < 10^3$ should be seriously considered.

Fig. 3 shows the same dependence but for $\Delta = 10^{-6}$. The ellipticity is substantially stronger even at a frequency $\omega/\omega_p \sim 10^2$.

Fig. 4 shows the dependence of the effect on the sign of η and $\bar{u}$ i.e. $\eta = 0.005$, $\bar{u} = 0.01$ (crosses), $\eta = 0.005$, $\bar{u} = -0.01$ (diamonds), $\eta = -0.005$, $\bar{u} = 0.01$ (triangles), $\eta = -0.005$, $\bar{u} = -0.01$ (circles). For this figure $\Delta = 10^{-6}$ and $\theta = 1°$. Note that the sense of the polarization depends on the sign of the parameters.

The sense of the polarization depends also on the magnitude of

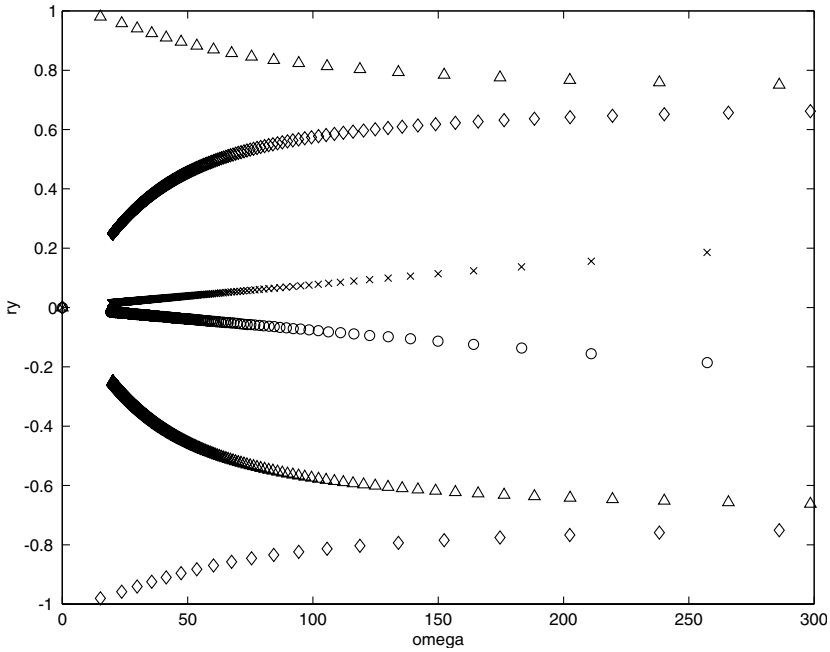

Figure 4. Ellipticity for $\Delta = 10^{-6}$, $\theta = 1°$, and various pairs of η and $\bar{u}$, i.e. $\eta = 0.005$, $\bar{u} = 0.01$ (crosses), $\eta = 0.005$, $\bar{u} = -0.01$ (diamonds), $\eta = -0.005$, $\bar{u} = 0.01$ (triangles), and $\eta = -0.005$, $\bar{u} = -0.01$ (circles).

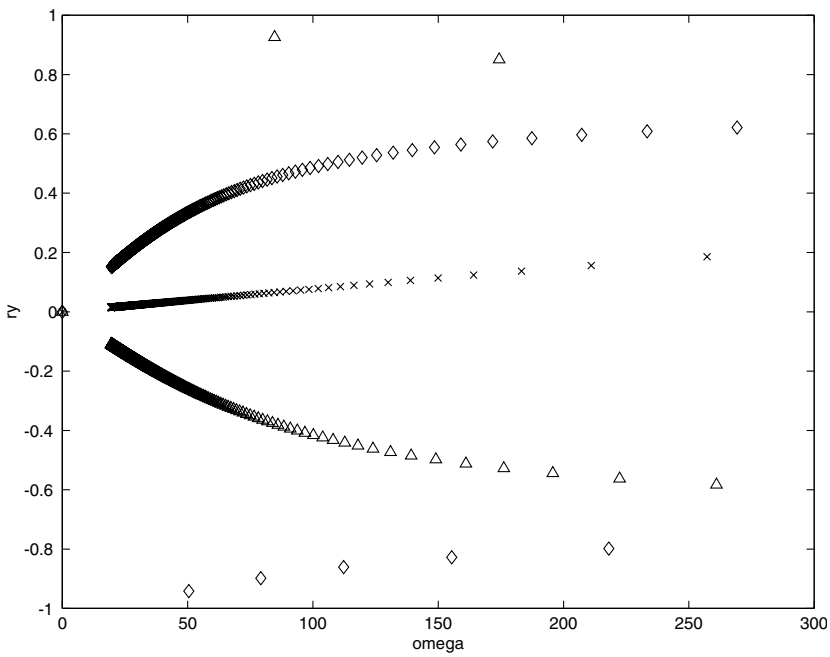

Figure 5. Ellipticity for $\Delta = 10^{-6}$, $\theta = 1°$, and two the following values of η and $\bar{u}$, i.e. $\eta = 0.005$, $\bar{u} = 0.01$ (crosses), $\eta = 0.01$, $\bar{u} = 0.01$ (diamonds), and $\eta = 0.005$, $\bar{u} = 0.02$ (triangles).

the parameters, as can be seen from Fig. 5, where we show the ellipticity for two different values of the parameter η and $\bar{u}$: $\eta = 0.005$, $\bar{u} = 0.01$ (crosses), $\eta = 0.01$, $\bar{u} = 0.01$ (diamonds), and $\eta = 0.005$, $\bar{u} = 0.02$ (triangles). In general, the sense of the polarization is determined by the sign of $d_{11}d_{22} - d_{12}^2$ [see equation (39)] which depends on the refraction index or frequency. For $|n^2 - 1| \ll \sin^2\theta \ll 1$, the sense of the polarization is determined by $\delta_2 - \delta_1$, that is, by the gyrotropic term ϵ_{12}.

7 EXAMPLE 1: POWER-LAW DISTRIBUTION IN THE PULSAR FRAME

Working in the plasma rest frame has the advantage of direct comparison with the conventional results of plasma physics, usually derived in the centre-of-mass frame. However, all analytically and numerically determined pair distributions are obtained in the pulsar frame. Moreover, consideration in the pulsar

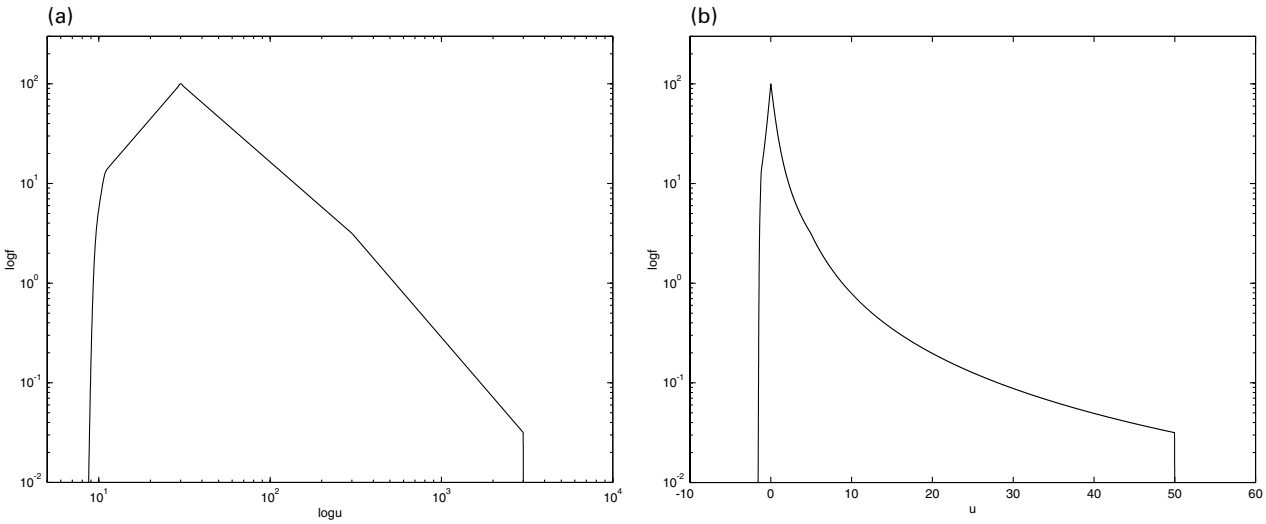

Figure 6. (a) The distribution numerically found by Daugherty & Harding (1982) in the pulsar frame. (b) The same distribution transformed in a frame moving with the velocity of the distribution maximum. Not normalized.

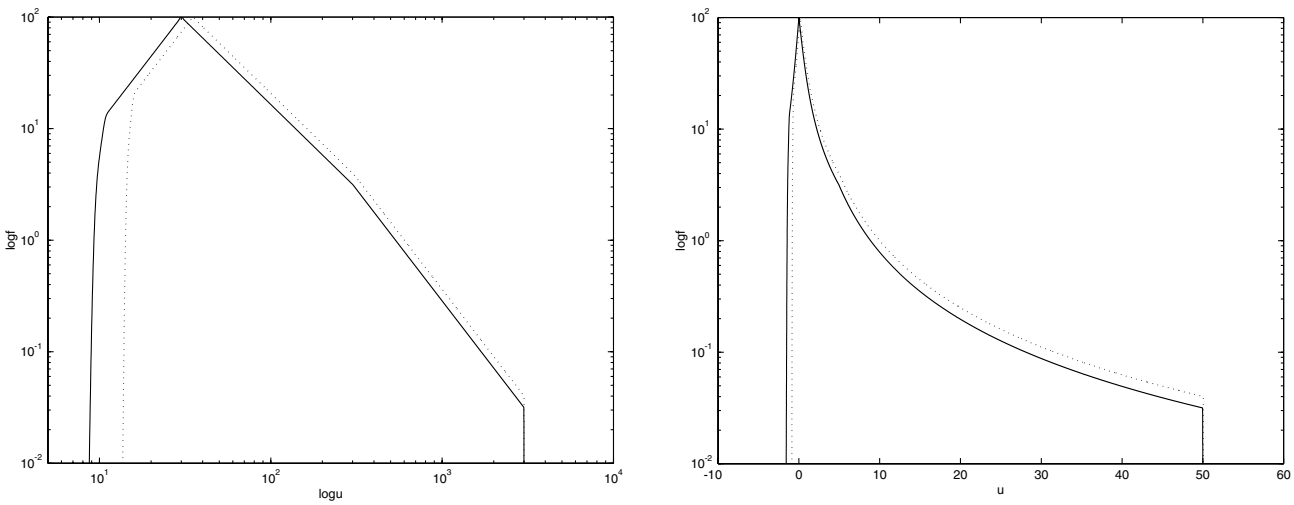

Figure 7. The two shifted distributions in the pulsar (a) and positron (b) frame. See explanation in text.

frame allows direct comparison with observations without any additional frame transformation. In this section we analyse the distribution of the kind:

$$f = \begin{cases} 0, & u < u_1 \\ f_m(\gamma/\gamma_2)^{\alpha_1}, & u_1 < u < u_2 \\ f_m(\gamma/\gamma_2)^{\alpha_2}, & u_2 < u < u_3\,. \\ f_m(\gamma_3/\gamma_2)^{\alpha_2}(\gamma/\gamma_3)^{\alpha_3}, & u_3 < u < u_4 \\ 0, & u_4 < u \end{cases} \tag{56}$$

A distribution of this shape was obtained by Daugherty & Harding (1982). The parameters derived from their fig. 7 are as follows (very approximately): $u_1 = 10$, $u_2 = 30$, $u_3 = 300$, and $u_4 = 3000$, while the multiplicity $M \sim 10^4$. These parameters are found for the Crab pulsar. For pulsars with periods around 0.5 s the multiplicity is $\sim 10^3$. The energies are also expected to be lower. The power spectra indices are $\alpha_1 \approx 2$, $\alpha_2 \approx -3/2$, and $\alpha_3 \approx -2$. The analytic fit for this distribution (smoothed by properly chosen tanh s) and its counterpart in the frame moving with the velocity u_2 is shown in Fig. 6. We choose such a distribution for both the positrons and electrons, normalizing them in the ratio $1 + \eta$ to $1 - \eta$, and with a relative drift $\bar{u} = u_+ - u_-$ applied to all $u_{1,2,3,4}$. Fig. 7 shows these distributions for the case where $\eta = 10^{-4}$ and $\bar{u} = -5$, so that in the pulsar frame the relative density and current are $\delta_1 = 2 \times 10^{-4}$ and $\delta_2 = 10^{-4}$, respectively. It is worth noting that the frame moving with a velocity u_2 is not the zero-bulk flow frame, which has $u_\mathrm{p} = 44.5$.

The angle $\theta = 5°$ in the plasma frame corresponds to an angle $\approx \theta/2\gamma_\mathrm{p} \approx 0\overset{\circ}{.}1$ in the pulsar frame. Fig. 8 shows the dependence of the frequency of the L mode on $n_\parallel - 1$ for different angles of propagation: circles stand for $\theta = 0\overset{\circ}{.}3$, diamonds for $\theta = 0\overset{\circ}{.}1$, triangles for $\theta = 0\overset{\circ}{.}03$, and crosses for $\theta = 0\overset{\circ}{.}001$. The parameter $\Delta = 10^{-5}$. The corresponding ellipticity is shown in Fig. 9. The ellipticity for $\theta = 0\overset{\circ}{.}3$ is negligible and is not shown. The ellipticity increases with increasing frequency and decreasing angle. For $\theta = 0\overset{\circ}{.}001$ the mode is completely circularly polarized at $\omega/\omega_\mathrm{p} > 40$. The transition from complete linear polarization to circular polarization (CP) is rather sharp. For larger angles of propagation, the elliptic polarization

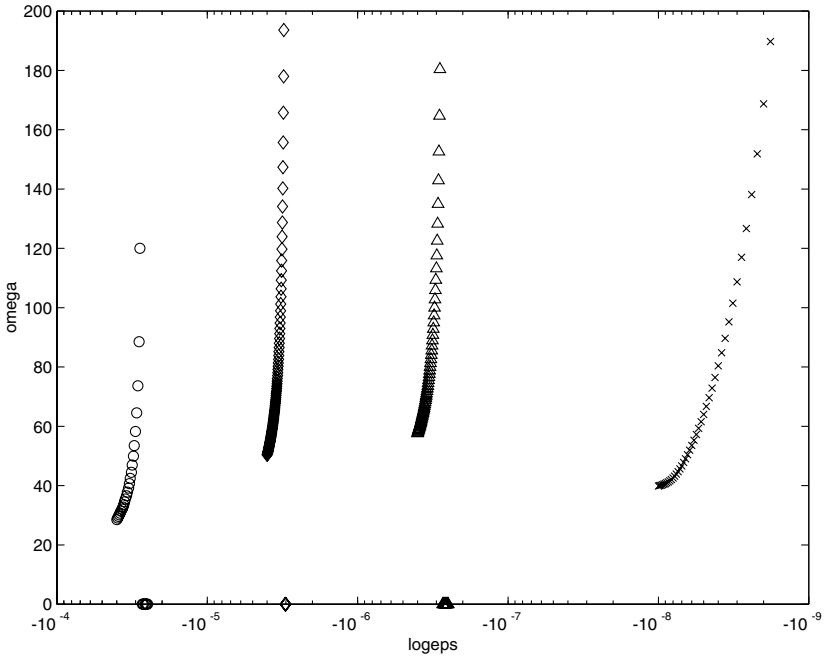

Figure 8. Frequency versus $n_{\parallel} - 1$ for $\Delta = 10^{-5}$ and various propagation angles, i.e. $\theta = 0\overset{\circ}{.}3$ (circles), $\theta = 0\overset{\circ}{.}1$ (diamonds), $\theta = 0\overset{\circ}{.}03$ (triangles), and $\theta = 0\overset{\circ}{.}001$ (crosses).

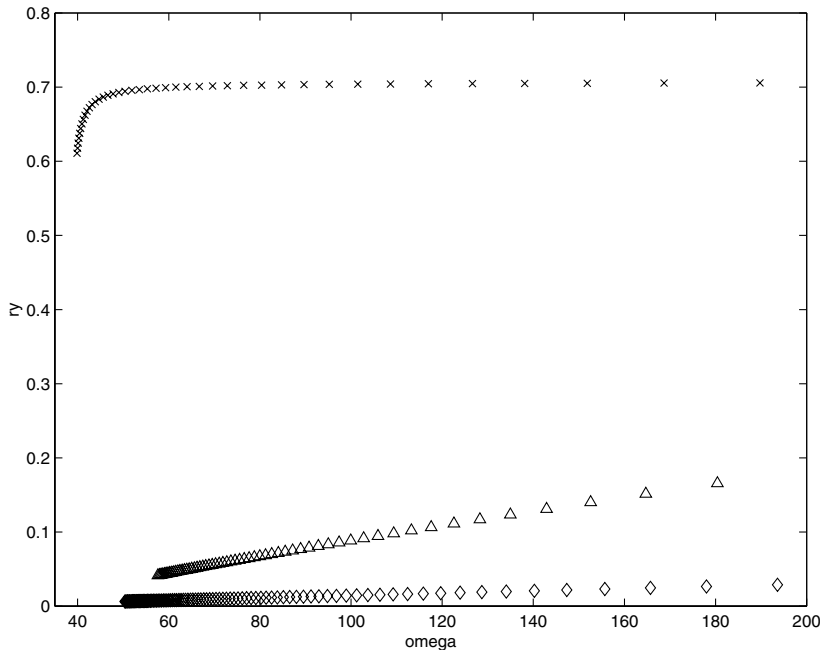

Figure 9. Ellipticity versus frequency for $\Delta = 10^{-5}$ and various propagation angles, i.e. $\theta = 0\overset{\circ}{.}1$ (diamonds), $\theta = 0\overset{\circ}{.}03$ (triangles), and $\theta = 0\overset{\circ}{.}001$ (crosses).

corresponds in fact to the transition region from the linear to CP, only this region is wide.

8 CP IN PULSAR RADIO EMISSION

Data on CP of pulsar radio emission has been reviewed (Han et al. 1998, 2000). In brief, Han et al. (2000) reported that: (i) CP can occur in both core and conal emission, (ii) it can reverse sense (handedness), not necessarily in the centre of the profile, (iii) there is no correlation with the position angle (PA) of the linear polarization for core emission, (iv) there is a strong correlation for conal emission between the sense of CP and the sign of the time derivation of PA (right hand CP and increasing PA), and (v) there is no systematic variation of CP with frequency, and many pulsars exhibit similar CP over a wide range of frequencies. These data refer to the CP averaged over many individual pulsars. In some cases the CP in individual pulsars is high and varies from pulse to pulse, such that the pulse-averaged CP is very much smaller than the characteristic CP in an individual pulse (Manchester, Taylor & Huguenin 1975; Stinebring et al. 1985). There is no entire satisfactory explanation for the origin of CP (Radhakrishnan & Rankin 1990; Kazbegi, Machabeli & Melikidze 1991;

Radhakrishnan 1992). The possible explanations can be separated into two classes: CP is intrinsic to the emission process, or is imposed as a propagation effect. The very high degree of CP in some individual pulses is difficult to reconcile with any possible pulsar emission mechanism, and we concentrate here on the possibilities of explaining the CP in terms of a propagation effect. There are several possibilities, most of which rely in some way on an electron–positron asymmetry.

We discuss one possibility: the emission occurs in a region where the modes are essentially linearly polarized, with the emission mechanism favouring one mode over the other. There is evidence that the radiation does escape as a mixture of two orthogonal wave modes, with opposite CPs, and that the net polarization depends on the ratio of the intensities in these two modes (McKinnon & Stinebring 2000). As the radiation propagates outward it should stay in its initial wave modes, as the properties of these modes, including the ellipticity of the polarization, change as the plasma parameters and the angle of propagation change. Our results show that the ellipticity depends strongly on the parameter ω_p/Ω, in the sense that CP is not significant when this parameter is too small. For example, for the power-law distribution in the pulsar frame (extending from $u_{\min} = 1$ to $u_{\max} = 300$, with the multiplicity $M \sim 10^4$, and with density and current parameters given by $\delta_1 = 2 \times 10^{-4}$ and $\delta_2 = 10^{-4}$, respectively), elliptical polarization is significant only for $\theta \lesssim 0\overset{\circ}{.}1$ in the pulsar frame. This range may be considered as the transition zone from the linear polarization regime (at larger angles) to the CP regime. CP dominates at angles $\sim 0\overset{\circ}{.}01$. This model implies that the natural modes are linear in the inner magnetosphere and elliptical only far from the surface at a distance of about 10^3 pulsar radii (depending on the plasma and magnetic field characteristics). If the radio spectrum forms well inside the magnetosphere, at $R \lesssim 10^2 R_p$ (Cordes 1992), the electromagnetic waves propagate outward initially as linearly polarized waves, evolving into (partly) circularly polarized waves as ω/ω_p, ω_p/Ω and θ change. At some point, called the polarization limiting region, the birefringence of the plasma becomes unimportant and polarization is fixed at that point.

The polarization limiting region (Cheng & Ruderman 1977; Petrova & Lyubarskii 2000), is where the characteristic distance, over which waves in the two modes get out of phase, becomes larger than the dimensions of the system. Specifically, it is where the difference between the refractive indices for the two (nearly degenerate almost electromagnetic) modes satisfies $|n_1 - n_2| \lesssim \lambda/L$, where λ is the wavelength and L is the typical scale of the plasma/magnetic field inhomogeneity (curvature). This condition implies the breakdown of the so-called adiabatic walking (Cheng & Ruderman 1977), where the local polarization is determined by the properties of the local modes in the approximation of geometrical optics. In order that significant CP be observed, the natural modes must be significantly elliptically polarized at the polarization limiting region (Cheng & Ruderman 1977). The location of the polarization limiting region depends on the propagation angle, the frequency, and on the inhomogeneity of the plasma (Arons & Barnard 1986; Petrova & Lyubarskii 2000). A detailed investigation is warranted, but is yet to be carried out.

As mentioned, there are several other ways in which CP can arise as a propagation effect. One way is through cyclotron damping. Cyclotron damping can affect the polarization by preferentially damping one mode compared with the other as the waves propagate through the region where the cyclotron resonance occurs (Kennett, Melrose & Luo 2001). Cyclotron damping is different for the two CPs whenever the distribution of electrons and positrons are not identical. Another possibility is that the radiation is scattered by inhomogeneities along the path of the ray, and such scattering leads to CPs that depends on the ellipticity of the natural modes in the scattering region, as well as on the details of the scattering. A systematic investigation of these and other possible causes for the CP is needed, and any such investigation will require a knowledge of the CP of natural modes and of its dependence on the plasma parameters.

9 CONCLUSIONS

We derive a general dispersion relation for low-frequency, $|\omega - k_\parallel v_\parallel| \ll \Omega/\gamma$, waves in a relativistic pair plasma with non-zero charge and current densities in the plasma, and with distributions of electrons and positrons in either the pulsar or plasma frames. The inclusion of non-zero charge and current densities imply that the natural wave modes are elliptically polarized. The ellipticity depends on the charge and current densities, denoted here by the parameters ρ/Ne and j/Nec, and also depends on both the wave frequency and angle of propagation. A motivation for this investigation is the interpretation of the CP of pulsar radio emission. Although the interpretation of CP remains unclear, a plausible explanation is that the radiation emerges in a mixture of the two natural wave modes, and that these are elliptically polarized due to the non-neutrality of the plasma. The results derived in this paper are needed for any systematic investigation of the interpretation of CP as a propagation effect.

ACKNOWLEDGMENTS

The authors are grateful to Yu. Lyubarsky for stimulating discussions and to Qinghuan Luo for helpful comments. This research was supported in part by Israel Science Foundation under the grant No. 170/00-1.

REFERENCES

Arons J., 1983, ApJ, 266, 175
Arons J., Barnard J. J., 1986, ApJ, 302, 120
Cheng A. F., Ruderman M. A., 1977, ApJ, 212, 800
Cordes J. M., 1992, in Hankins T. H., Rankin J. M., Gill J. A., eds, The Magnetospheric Structure and Emission Mechanisms of Radio Pulsars. Pedagogical Univ. Press, Zielona Góra, Poland, p. 253
Daugherty J. K., Harding A. K., 1982, ApJ, 252, 337
Gangadhara R. T., 1997, A&A, 327, 155
Gedalin M. E., Machabeli G. Z., 1982, SvA. Lett., 8, 153
Gedalin M., Melrose D. B., Gruman E., 1998, Phys. Rev. E, 57, 3399
Gil J. A., Snakowski J. K., 1990a, A&A, 234, 237
Gil J. A., Snakowski J. K., 1990b, A&A, 234, 269
Han J. L., Manchester R. N., Xu R. X., Qiao G. J., 1998, MNRAS, 300, 373
Han J. L., Manchester R. N., Qiao G. J., 2000, in Kramer M., Wex N., Wielebinski R., eds, Proc. IAU Colloq. 177 Pulsar Astronomy – 2000 and Beyond. Astron. Soc. Pac., San Francisco, p. 251
Kazbegi A. Z., Machabeli G. Z., Melikidze G. I., 1991, MNRAS, 253, 377
Kennett M. P., Melrose D. B., Luo Q., 2001, J. Plasma Phys., in press
Lominadze J. G., Mikhailovskii A. B., Sagdeev R. Z., 1979, Zh. Eksp. Teor. Fiz., 77, 1951
Lominadze J. G., Machabeli G. Z., Usov V. V., 1983, Ap&SS, 90, 19
Lyubarskii Y. E., 1992, A&A, 265, L33
Lyubarskii Yu. E., 1995, Astrophys. Space Phys. Rev., 9, 1
Lyubarskii Y. E., Petrova S. A., 1999, Ap&SS, 262, 379
Lyutikov M., 1998, MNRAS, 293, 447
Lyutikov M., 1999, ApJ, L37, 525

Lyutikov M., Machabeli G., Blandford R., 1999, ApJ, 512, 804
Manchester R. N., Taylor J. H., 1977, Pulsars. Freeman, San Francisco
Manchester R. N., Taylor J. H., Huguenin G. R., 1975, ApJ, 196, 83
Manchester R. N., Han J. L., Qiao G. J., 1998, MNRAS, 295, 280
McKinnon M. M., Stinebring D. R., 2000, ApJ, 529, 435
Melrose D. B., 1993, in Blandford R. D., Hewish A., Lyne A. G., Mestel L., eds, Pulsars as Physics Laboratories. Oxford Univ. Press, Oxford, p. 105
Melrose D. B., 1995, JA&A, 16, 137
Melrose D. B., Gedalin M., Kennett M. P., Fletcher C. S., 1999, J. Plasma Phys., 62, 233
Petrova S. A., Lyubarskii Y. E., 2000, A&A, 355, 1168
Radhakrishnan V., 1992, in Hankins T. H., Rankin J. M., Gil J. A., eds, Proc. IAU Symp. 128, The magnetospheric structure and emission mechanisms of radio pulsars. Pedagogical Univ. Press, Zielona Góra, p. 367
Radhakrishnan V., Rankin J. M., 1990, ApJ, 352, 822
Ruderman M. A., Sutherland P. G., 1975, ApJ, 196, 51
Shibata S., Miyazaki J., Takahara F., 1998, MNRAS, 295, L53
Stinebring D. R., Cordes J. M., Weisberg J. M., Rankin J. M., Boriakoff V., 1985, ApJS, 55, 247
Usov V. V., 1987, ApJ, 320, 333
Volokitin A. S., Krasnoselskikh V. V., Machabeli G. Z., 1985, Sov J. Plasma Phys. Plasma Phys., 11, 531
von Hoensbroech A., Lesch H., 1999, A&A, 342, L57
von Hoensbroech A., Kijak J., Krawczyk A., 1998, A&A, 334, 571
Zhang B., Harding A. K., 2000, ApJ, 532, 1150

This paper has been typeset from a TEX/LATEX file prepared by the author.